Virtual Coupling Train Following Control Using High Order Control Barrier Functions

Yike Li, Yin Tong , Alessandro Giua

***Abstract*— Virtual Coupling (VC) has gained increasing attention as a next-generation railway signaling solution. Its implementation, however, poses critical control challenges, as following trains must maintain small inter-train spacing under dynamic operating conditions. This paper proposes a decentralized control framework for VC followers, where safety is defined by the relative braking distance (RBD) principle and enforced through High Order Control Barrier Functions (HOCBFs). An adaptive switching heuristic is introduced to compute the reference control force while accounting for potential Train-to-Train (T2T) communication delays. The HOCBF constraints and reference control are embedded into a sequence of Quadratic Programs (QPs) solvable in real time. The proposed method guarantees safety for VC followers without requiring centralized coordination or full trajectory prediction of the preceding trains.**

I. INTRODUCTION

To meet the growing demand for railway capacity, Virtual Coupling (VC) has emerged as a promising signaling concept that enables trains to dynamically form convoys and separate, thereby improving operational flexibility without the need for physical couplers [1]. In a VC convoy, multiple trains operate at a reduced spacing and coordinate their movements through Train-to-Train (T2T) wireless communication. This enables flexible train formations based on real-time passenger or freight demands, while avoiding issues associated with traditional mechanical coupling—such as incompatibility between heterogeneous carriages and excessive in-train forces [2]. Recent studies have demonstrated that VC can significantly reduce headway and enhance line throughput [3].

Among previous studies on train control under VC, the general idea is to control the follower's velocity based on the distance to its predecessor. Traditional moving block systems use the absolute braking distance [4], In contrast, VC leverages T2T communication to enable the more efficient *relative braking distance* (RBD) principle [5], which considers the braking performance of both follower and predecessor and effectively reduces unnecessary gaps between them. Despite the RBD principle being the theoretical basis for VC spacing, many studies adopt a simplified version of the RBD usually in the following three different ways: (i) constant minimum distances, (ii) linearized RBD-based distances and (iii) scenario-based distances.

Constant spacing is often set empirically, e.g., 130 m in [6], 200–300 m in [7], or 60 m in [8]. Such values are acceptable for high-speed lines. However, they are impractical for metro lines. Metro platforms are shorter, and stations are closer together, where closely coupled operations are crucial to adapt to fluctuating passenger demand and improve service quality. The linearized RBD proposed in [9], [10] assume identical braking rates and velocity limits, which simplifies control but ignores potential safety risks. Some studies utilize constant time headway to define the linear spacing principle [11], which is originated from the autonomous cruise control of cars. However, this criterion of cars lacks practical validation in the railway context, where braking dynamics of train differ significantly from that of road vehicles. Scenario-based spacing approaches adjust the minimum separation according to discrete operational phases [12], [13]. An additional scheme is required to identify and manage those different phases, which might increase system complexity.

On the other hand, the train-borne implementation of VC functionality primarily requires upgrading the onboard system, which must meet strict safety and real-time computing requirements. Once the formation is established, the leading train handles path planning. The key challenge in controlling a following train lies in ensuring both safety and stability while responding to the leader's maneuvers and satisfying time-varying constraints. This motivates the need for real-time capable control algorithms that can guarantee safety without compromising the capacity benefits enabled by VC.

To address the identified research gaps, this paper proposes a HOCBF-based optimal safety controller for the following trains in VC. Control Barrier Function (CBF) are Lyapunov-like functions that enforce state-dependent constraints on the control input, ensuring that the system remains within a predefined safe set. CBFs have recently emerged as powerful tools for safety-critical control of dynamical systems, and have been successfully applied to real-time control in applications such as drones, bipedal robots, and connected autonomous vehicles [14]. High Order Control Barrier Functions (HOCBFs), as a generalization of CBFs,

This work has been supported by the project co-funded by the European Union – Next Generation Eu - under the National Recovery and Resilience Plan (NRRP), Mission 4 Component 1 Investment 4.1 - Decree No.351 (9th April 2022) of Italian Ministry of University and Research - Concession Decree No. 2152 (28th December 2022) of the Italian Ministry of University and Research, Project code D93C22000860005, within the Italian National Program PhD Programme in Autonomous Systems (DAuSy), by the Project SERICS (PE00000014), and by the National Natural Science Foundation of China under Grant No. 62373313 and by the Fundamental Research Funds for the Central Universities under Grant No. 2682025GH015.

Y. Li is with the Department of Electrical and Electronic Engineering, University of Cagliari, Cagliari 09123, Italy; and the Department of Electrical and Information Engineering, Polytechnic of Bari, Bari 70125, Italy yike.li@unica.it; y.li@phd.poliba.it

Y. Tong (*Corresponding Author) is with the School of Information Science and Technology, Southwest Jiaotong University, Chengdu 611756, China yintong@swjtu.edu.cn

A. Giua is with the Department of Electrical and Electronic Engineering, University of Cagliari, Cagliari 09123, Italy giua@unica.it

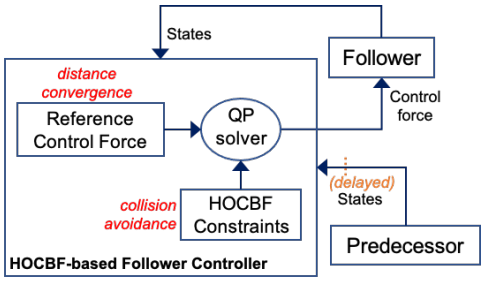

Fig. 1: Framework of the HOCBF-based VC Follower Controller.

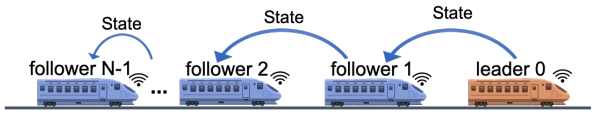

Fig. 2: A general VC convoy consisting of N trains.

are specifically designed to handle constraints with arbitrary relative degree [15].

The overall controller design is depicted in Fig. 1. Combining the kinetic information transmitted from the preceding train via T2T communication, a reference control force is computed to achieve convergence in inter-train distance. An adaptive switching mechanism is employed to account for potential T2T communication delays. Meanwhile, HOCBFs are formulated to enforce collision avoidance constraints by filtering the reference force. The controller integrates the reference force and HOCBF constraints into a Quadratic Program (QP) to compute the control input. A decentralized control scheme is adopted, where each follower solves its local QP based on the proposed HOCBF-based framework.

The main contributions of this paper are: 1. A realization of the RBD-based spacing policy using HOCBFs, enhancing the flexibility of convoy movement. 2. A real-time controller capable of handling time-varying leader maneuvers and communication delays. The remainder is organized as follows. Section II introduces the VC train following control problem. Section III presents the control approach. Effectiveness of the proposed approach is demonstrated with a simulation in Section IV. Conclusion is given in Section V.

II. Problem Formulation

In this section, we first provide a brief overview of the decentralized control scheme for a VC convoy and the train dynamics, then formalize the constraints and objectives of the following train control problem.

A. Convoy Structure and Train Dynamics

We investigate a general VC convoy consisting of N trains as shown in Fig. 2, where each following train i ($i = 1, 2, \ldots, N-1$), simply called the follower, receives real-time kinematic data (e.g., speed, position, acceleration) only from its direct predecessor $i-1$. The leading train (simply called the leader), indexed by 0, is responsible for processing operational commands that determine the overall convoy behavior, such as entering and departing one segment or stations. Each follower adjust its control input to maintain the desired spacing and velocity relative to its preceding train.

In this paper, we focus on the control of following trains and assume that the trajectory of the leading train has been pre-designed. The longitudinal dynamics of each follower i can be modeled as a mass-point system and is described by the following continuous dynamic equation [16]:

$$\begin{cases} \dot{p}_i(t) = v_i(t) \\ \dot{v}_i(t) = \dfrac{u_i(t) - r_i(t)}{M_i} \end{cases} \tag{1}$$

where M_i [kg] denotes the mass of train i, $v_i(t)$ [m/s] is the velocity, and $p_i(t)$ [m] is the position of the train's head. External forces include the traction or braking force (T/B force) $u_i(t)$ [N], which is the control input, and the running resistance force $r_i(t)$ [N] is calculated by a 2-order empirical equation called the Davis equation [17]:

$$r_i(t) = (C_{0,i} + C_{1,i} v_i(t) + C_{2,i} v_i^2(t)) M_i, \tag{2}$$

where $C_{1,i}$ and $C_{2,i}$ are the coefficients related to mechanical and aerodynamic characteristics, respectively. The parameter $C_{0,i}$ refers to the starting resistance, which can be neglected when the speed is greater than 3 m/s.

B. Constraints and Objectives

To ensure safety and stability of the convoy movement, the following constraints are defined.

1) Control Limits: The control input $u_i(t)$ is constrained by the mechanical limitations:

$$-M_i B_i \le u_i(t) \le M_i T_i, \tag{3}$$

where $B_i > 0$ and $T_i > 0$ denote the maximum allowable braking and traction rates (in m/s^2), respectively.

2) Collision Avoidance Constraint: Let $d_i(t)$ be the distance between the head of train i and the rear of train $i-1$, given by

$$d_i(t) = p_{i-1}(t) - p_i(t) - L_{i-1}, \tag{4}$$

where $p_{i-1}(t)$ and $p_i(t)$ denote the head positions of the two trains, and L_{i-1} is the length of train $i-1$. To ensure safety under all braking scenarios, the distance between train i and train $i-1$ must always be greater than or equal to a *minimum safe distance* $d_i^*(t)$ determined by the RBD-based spacing principle:

$$d_i(t) \ge d_i^*(t) = \max(\theta_i(t), 0) + d_0, \tag{5}$$

where d_0 is a default margin that separates trains even when they are both stationary, ensuring a standstill clearance, and $\theta_i(t)$ represents the deviation between the braking distances of train i and train $i-1$, given by

$$\theta_i(t) = \frac{v_i(t)^2}{2SB_i} - \frac{v_{i-1}(t)^2}{2EB_{i-1}}. \tag{6}$$

The operator $max(\cdot)$ ensures that, for the case $\theta_i(t) < 0$, $d_i^*(t) = d_0$. In (6), SB_i denotes the service braking rate of train i, and EB_{i-1} is the emergency braking rate of train $i-1$, with $SB_i < EB_{i-1}$.

3) Convoy Convergence Objective: In traditional optimization control for train convoys, the convergence objective involves minimizing tracking errors in both spacing and velocity. In this work, we focus on spacing convergence, as it directly determines the convoy's compactness and safety. By (5) and (6), $d_i^*(t)$ increases quadratically with velocity while decreases as the convoy slows down. For example, a 50 m/s convoy requires a minimum safe spacing of 138 m (assuming $SB_i = 1.5\ \mathrm{m/s^2}$, $EB_{i-1} = 1.8\ \mathrm{m/s^2}$), which will reduce to 22 m at the velocity of 20 m/s. Let $\delta_i^d(t) = d_i(t) - d_i^*(t)$ be the spacing deviation. To increase the line capacity, it is necessary to minimize the space between trains as much as possible. Therefore, the convoy convergence goal is

$$\lim_{t\to\infty} \delta_i^d(t) = 0. \tag{7}$$

Remark: We do not limit the maximum value of $\delta_i^d(t)$, because a large spacing intrinsically offers additional safety. Moreover, excessive distance does not necessarily disrupt VC: recent T2T communication technologies indicate reliable performance even if the trains are separated up to 10 km [18].

III. Controller Design

To design the controller for each following train i, we combine the above proposed constraint and objective with the train dynamics to establish the train control model.

A. Follower Model

1) Nominal model: To compute the control force for each following train in the VC convoy, we model the train i as a nonlinear affine control system. Let $\boldsymbol{x}_i(t) = [p_i(t), v_i(t)]^\top$, based on the longitudinal dynamics (1),

$$\underbrace{\begin{bmatrix}\dot{p}_i(t)\\ \dot{v}_i(t)\end{bmatrix}}_{\dot{\boldsymbol{x}}_i(t)} = \underbrace{\begin{bmatrix}v_i(t)\\ -\frac{r_i(t)}{M_i}\end{bmatrix}}_{f(\boldsymbol{x}_i(t))} + \underbrace{\begin{bmatrix}0\\ \frac{1}{M_i}\end{bmatrix}}_{g(\boldsymbol{x}_i(t))} u_i(t). \tag{8}$$

Ideally, the following train receives real-time information from the preceding train through constant and reliable T2T communication. This work considers the presence of the occasional communication delay with a permissive range, proposing a heuristic to process the delay, with the goal of mitigating their impact and avoiding undesirable actions that may compromise VC performance, such as emergency braking or system degradation.

2) Communication delay: The transmitted packet includes the preceding train's position and velocity $\boldsymbol{x}_{i-1}$, as well as its acceleration a_{i-1}, which can be grouped into the state vector

$$\Psi_{i-1}(t) = [p_{i-1}(t),\ v_{i-1}(t),\ a_{i-1}(t)]^\top.$$

The T2T channel is modeled as a FIFO buffer. When a delay τ occurs at time t', no updated packet arrives from train $i-1$ during $[t',\ t'+\tau)$. After τ, the system resumes receiving packets, but the information is delayed until the delay is cleared (by the communication module) at time t''. With embedded timestamps, train i is able to detect τ upon the first delayed packet at $t'+\tau$, and determine t'' exactly when a packet arrives with its send-time stamp that equals to t''. Assuming $t'' > t'+\tau$, the received state vector under delay $\hat{\Psi}_{i-1}(t) = [\hat{p}_{i-1}(t),\ \hat{v}_{i-1}(t),\ \hat{a}_{i-1}(t)]^\top$ is defined as

$$\hat{\Psi}_{i-1}(t) = \begin{cases}\Psi_{i-1}(t'), & t \in [t',\ t'+\tau),\\ \Psi_{i-1}(t-\tau), & t \in [t'+\tau,\ t''),\\ \Psi_{i-1}(t), & \text{otherwise.}\end{cases} \tag{9}$$

We model the delay τ as a constant bounded by the maximum value $\tau_{\max} = 400$ ms. For simplicity, this paper studies the case where is only one communication delay in the control horizon. It is worth noting that the proposed method can be applied to the scenarios that may have multiple delays with different values in $[0,\ \tau_{\max}]$.

B. Reference Control Force

The reference solution is based on the convoy convergence goal (7), i.e. to minimize the spacing distance.

1) Nominal design: Given $\delta_i^d(t) \geq 0$, we compute a *reference acceleration* $a_i^*(t)$ for train i such that in the time interval ϵ_c, distance deviation δ_i^d goes to 0 at time $t+\tau$. Assume that train $i-1$ maintains the current acceleration $a_{i-1}(t)$, this occurs when the following formula (10) holds

$$\left(v_i(t)\epsilon_c + \frac{a_i^*(t)\epsilon_c^2}{2}\right) - \left(v_{i-1}(t)\epsilon_c + \frac{a_{i-1}(t)\epsilon_c^2}{2}\right) = \delta_i^d(t) \tag{10}$$

where the first element represents the distance traveled by train i over ϵ_c with the recommended acceleration $a_i^*(t)$. The second represents the distance traveled by train $i-1$ over the same period ϵ_c with its current acceleration $a_{i-1}(t)$. The relative displacement between train i and train $i-1$ compensates the spacing deviation δ_i^d.

From (10), the reference acceleration for train i is obtained by

$$a_i^*(t) = \frac{2}{\epsilon_c^2}\,\delta_i^d(t) + \frac{2}{\epsilon_c}\,(v_{i-1}(t) - v_i(t)) + a_{i-1}(t). \tag{11}$$

In (11), ϵ_c is defined as the *convergence time*, representing the time period over which train i adjusts its state to reduce δ_i^d and achieve the desired spacing relative to train $i-1$.

2) In the presence of τ: The reference acceleration under delay is computed based on the availability of the received information, as given in (9). Specifically, during the delay period $t \in [t',\ t'']$, it is determined by the sign of the received (delayed) predecessor acceleration $\hat{a}_{i-1}(t)$ as follows:

- If $\hat{a}_{i-1}(t) \geq 0$, the following train maintains its velocity (i.e., cruises).
- If $\hat{a}_{i-1}(t) < 0$, the following train applies service braking.

Once the delay period ends, the computation reverts to the nominal logic defined in (11). To summarize, the *delay-aware reference acceleration*, denoted by $\hat{a}_i^*(t)$, is defined as

$$\hat{a}_i^*(t) = \begin{cases}0, & t \in [t',\ t''] \text{ and } \hat{a}_{i-1}(t) \geq 0,\\ -SB_i, & t \in [t',\ t''] \text{ and } \hat{a}_{i-1}(t) < 0,\\ a_i^*(t), & \text{otherwise.}\end{cases} \tag{12}$$

This adaptive strategy avoids reliance on motion prediction of the preceding train, while ensuring safety without triggering unnecessary emergency braking. By preserving convoy spacing to the extent allowed by delayed information, it maintains VC functionality under occasional communication delay.

Furthermore, $\hat{a}_i^*(t)$ is saturated by the admissible limits (3), which is given by

$$u_i^{\text{ref}}(t) = \text{sat}\big((M_i\hat{a}_i^*(t) + r_i(t)),\ -M_iB_i,\ M_iT_i\big), \tag{13}$$

where the saturation function $\text{sat}(\cdot)$ is defined as:

$$\text{sat}(u,\ -M_iB_i,\ M_iT_i) = \begin{cases} -M_iB_i, & \text{if } u < -M_iB_i, \\ u, & \text{if } -M_iB_i \le u \le M_iT_i, \\ M_iT_i, & \text{if } u > M_iT_i. \end{cases}$$

C. Collision Avoidance with HOCBFs

Essentially, HOCBFs can map the constraints from the system states $\boldsymbol{x}_i(t)$ to the control input $u_i(t)$. In order to enforce the collision avoidance constraint (5), we construct the HOCBF constraints in this section. For further technical details of HOCBFs, see [15].

To account for the possible existence of a delay τ, we redefine the relevant variables by incorporating the received predecessor states $\hat{\Psi}_{i-1}(t)$ as defined in (9). Specifically, we denote the delay-aware distance and braking difference as $\hat{d}_i(t) = \hat{p}_{i-1}(t) - p_i(t)$ and $\hat{\theta}_i(t) = \frac{v_i(t)^2}{2SB_i} - \frac{\hat{v}_{i-1}(t)^2}{2EB_{i-1}}$. The corresponding minimum safe distance is given by $\hat{d}_i^*(t) = \max(\hat{\theta}_i(t),\ 0) + d_0$, and the resulting spacing deviation is $\hat{s}_i^d(t) = \hat{d}_i(t) - \hat{d}_i^*(t)$. Consequently, the collision avoidance constraint can be reformulated as

$$\hat{s}_i^d(t) = \hat{d}_i(t) - \max(\hat{\theta}_i(t),\ 0) - d_0 \ge 0. \tag{14}$$

Note that the operator $\max(\cdot, 0)$ is nondifferentiable at zero, whereas the HOCBF must be defined as a continuously differentiable function. To overcome this problem, we define two HOCBF candidates:

$$b_1(\boldsymbol{x}_i(t), t) = \hat{d}_i(t) - \hat{\theta}_i(t) - d_0, \tag{15}$$

$$b_2(\boldsymbol{x}_i(t), t) = \hat{d}_i(t) - d_0. \tag{16}$$

Intuitively, we have

$$\hat{s}_i^d(t) = \min\big(b_1(\boldsymbol{x}_i(t), t),\ b_2(\boldsymbol{x}_i(t), t)\big).$$

Therefore, the constraint $\hat{s}_i^d(t) \ge 0$ holds if and only if both $b_1(\boldsymbol{x}_i(t), t) \ge 0$ and $b_2(\boldsymbol{x}_i(t), t) \ge 0$. In other words, enforcing $b_1(\boldsymbol{x}_i(t), t) \ge 0$ and $b_2(\boldsymbol{x}_i(t), t) \ge 0$ simultaneously is thus equivalent to enforcing the original constraint (14).

Here, the arguments of $b_1(\boldsymbol{x}_i(t), t)$ and $b_2(\boldsymbol{x}_i(t), t)$ explicitly state both $\boldsymbol{x}_i(t)$ and t, since they depends not only on the states of train i but also on the time-varying states of preceding train $i-1$. For simplicity, in the following we omit the time dependency of variables except for the HOCBFs.

To construct the constraint corresponding to $b_1(\boldsymbol{x}_i, t)$, we choose the quadratic class $\mathcal{K}$ function,

$$\dot{b}_1(\boldsymbol{x}_i, t) + b_1^2(\boldsymbol{x}_i, t) \ge 0, \tag{17}$$

where

$$\begin{aligned}\dot{b}_1(\boldsymbol{x}_i, t) &= \frac{\partial b_1(\boldsymbol{x}_i, t)}{\partial \boldsymbol{x}_i(t)} \cdot \frac{d\boldsymbol{x}_i}{dt} + \frac{\partial b_1(\boldsymbol{x}_i, t)}{\partial t} \\ &= \begin{bmatrix} -1 & -\frac{v_i}{SB} \end{bmatrix} \dot{\boldsymbol{x}}_i + \hat{v}_{i-1} + \frac{\hat{v}_{i-1}\hat{a}_{i-1}}{EB_{i-1}}.\end{aligned}$$

Substituting $\dot{\boldsymbol{x}}_i$ from (8), and further substituting in (17) (detailed steps omitted), the control constraint is derived as:

$$\begin{aligned}&-\frac{v_i}{M_i\,SB_i}u_i + \big(\frac{r_i}{M_i\,SB_i} - 1\big)v_i \\ &+\big(\frac{\hat{a}_{i-1}}{EB_{i-1}} + 1\big)\hat{v}_{i-1} + b_1^2(\boldsymbol{x}_i, t) \ge 0,\end{aligned} \tag{18}$$

which is affine in u_i. All values of u_i satisfying (18) ensure that $b_1(\boldsymbol{x}_i(t), t) \ge 0$ holds.

For $b_2(\boldsymbol{x}_i, t)$, the auxiliary functions employing the quadratic class $\mathcal{K}$ function are defined as

$$\begin{aligned}\psi_0(\boldsymbol{x}_i, t) &= b_2(\boldsymbol{x}_i, t), \\ \psi_1(\boldsymbol{x}_i, t) &= \dot{\psi}_0(\boldsymbol{x}_i, t) + \psi_0^2(\boldsymbol{x}_i, t)\end{aligned}$$

and the HOCBF $b_2(\boldsymbol{x}_i, t)$ should satisfy

$$\dot{\psi}_1(\boldsymbol{x}_i, t) + \psi_1(\boldsymbol{x}_i, t)^2 \ge 0. \tag{19}$$

By substituting, inequality (19) becomes

$$\begin{aligned}&\ddot{b}_2(\boldsymbol{x}_i, t) + 2\dot{b}_2(\boldsymbol{x}_i, t)\, b_2(\boldsymbol{x}_i, t) \\ &\quad +\big(\dot{b}_2(\boldsymbol{x}_i, t) + b_2^2(\boldsymbol{x}_i, t)\big)^2 \ge 0,\end{aligned} \tag{20}$$

where

$$\dot{b}_2(\boldsymbol{x}_i, t) = \hat{v}_{i-1} - v_i,$$

and

$$\ddot{b}_2(\boldsymbol{x}_i, t) = \hat{a}_{i-1} - \dot{v}_i.$$

The resulting control constraint is given by

$$\begin{aligned}&-\frac{1}{M_i}u_i + \frac{r_i}{M_i} + \hat{a}_{i-1} + 2(\hat{v}_{i-1} - v_i)b_2(\boldsymbol{x}_i, t) \\ &\quad +\big(\hat{v}_{i-1} - v_i + b_2^2(\boldsymbol{x}_i, t)\big)^2 \ge 0.\end{aligned} \tag{21}$$

D. Decentralized VC Follower Optimal Control

Our goal is to determine the control input to achieve the distance convergence subject to RBD constraints. To minimizing the deviation from the reference control force in (13), the QP of train i is constructed by combining the above HOCBF constraints as

$$\begin{aligned}u_i(t) = \arg\min &\left(H_i(u_i(t) - u_i^{\text{ref}}(t))^2\right) \\ \textbf{s.t.}\quad &\text{Train dynamic (8), control limit (3)} \\ &\text{HOCBF constraints (18), (21),}\end{aligned} \tag{22}$$

where the scalar H_i is the quadratic cost weight. In practice, time is discretized with step size dt, and a QP with HOCBF constraints for each follower is solved at each time step k. Afterwards, the control from solving the QP is held constant and is applied at the current time step. The detailed procedure of the decentralized safe optimal control for the VC followers is summarized in the following Algorithm.

Algorithm: Decentralized VC Follower Safe Optimal Control

1: Initialize the states $\boldsymbol{x}_i$ for all followers $i = 1, \ldots, N-1$
2: **for** each time step $k = 1, \ldots, K = t_f/dt$ **do**
3: **for** each follower $i = 1, \ldots, N-1$ **do**
4: Acquire predecessor's information $\hat{\Psi}_{i-1}(k)$
5: Compute reference control force $u_i^{\text{ref}}(t)$ via Eq. (13)
6: Formulate HOCBF constraints via Eqs. (18) and (21)
7: Solve QP in Eq. (22) to get optimal input $u_i(t)$
8: **end for**
9: **for** each follower $i = 1, \ldots, N-1$ **do**
10: Update state $\boldsymbol{x}_i(k+1)$ with $u_i(k)$ through Eq. (8)
11: **end for**
12: **end for**

TABLE I: Parameters of Train Dynamics

Parameter	Value	Unit
$M_0,\ M_1,\ M_2$	383,000	kg
$L_0,\ L_1,\ L_2$	100	m
$C_{0,0},\ C_{0,1},\ C_{0,2}$	0.01176	N/kg
$C_{1,0},\ C_{1,1},\ C_{1,2}$	0.00077616	Ns/m·kg
$C_{2,0},\ C_{2,1},\ C_{2,2}$	1.6×10^{-5}	$\text{Ns}^2/\text{m}^2\cdot\text{kg}$
$SB_0,\ SB_1,\ SB_2$	1.5	m/s^2
$EB_0,\ EB_1,\ EB_2$	1.8	m/s^2
$B_0,\ B_1,\ B_2$	2	N/kg
$T_0,\ T_1,\ T_2$	2	N/kg

Remark: While $u_i^{\text{ref}}(t)$ offers a relatively large feasible region prior to HOCBF activation, this work does not explicitly guarantee the feasibility of the QP under all operating conditions. A promising approach is to incorporate a slack variable into the HOCBF constraints, which could also effectively address model uncertainties in future extensions.

IV. Simulation and Case Study

To evaluate the effectiveness of the proposed control method, we conduct simulations on a VC convoy of three trains (Train 0, 1, and 2). Detailed dynamic parameters of the trains are listed in Table I. We set the default margin $d_0 = 10$ m, and the convergence time $\epsilon_c = 5$ s. The convoy starts from rest, with each pair of adjacent trains initially spaced by default margin d_0. A predefined trajectory is assigned to Train 0, which undergoes an acceleration–cruise–deceleration process as it approaches the destination.

• *Nominal Case: No Delay*

We first investigate a nominal case without communication delay. Performing the simulation of 200 s with the step size 0.02 s, the simulation results[1] are shown in Fig. 3. From Fig. 3a, we can see that, in the nominal case, the convoy undergoes acceleration, cruising, and deceleration, during which Train 1 and Train 2 closely follow the trajectory of Train 0. As shown in Fig. 3b, the actual inter-train distances $d_1(t)$ and $d_2(t)$ remain above and closely follow the corresponding safe distances $d_1^*(t)$ and $d_2^*(t)$ (dashed lines in the figure), with deviations within 15 m. The inter-train distances converge smoothly to the desired default spacing d_0 at standstill. A temporary increase in the deviation $d_1(t) - d_1^*(t)$ is observed when Train 0 starts braking at 102 s, as the safety distance $d_1^*(t)$

[1]The QPs are solved using Matlab toolbox `quadprog`. The obtained closed loop system is simulated using function `ode45`.

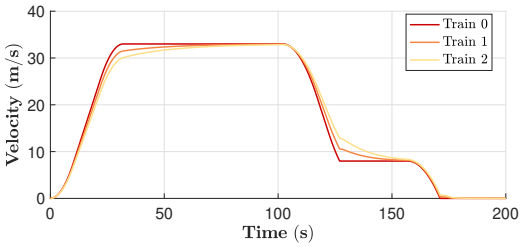

(a) Train velocity profile. The convoy undergoes a journey consisting of acceleration, cruise, and deceleration.

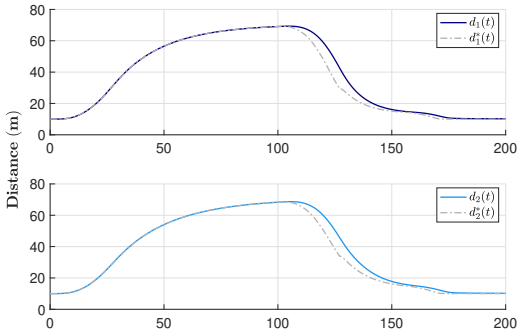

(b) Inter-train distance over time. The actual distance (solid line) throughout the entire journey is greater than and close to the desired distance (dash line).

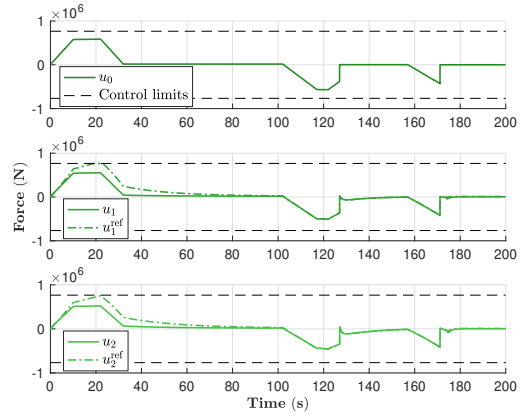

(c) Control force over time. The deviations between reference force and actual force indicates the activation of HOCBF.

Fig. 3: Results of the delay-free case.

rapidly increases due to the HOCBF's immediate response to the drop in $v_0(t)$. This braking event also affects the following pair, leading to a similar but milder deviation in $d_2(t) - d_2^*(t)$. Upon stopping, the inter-train distances are effectively reduced to the desired default spacing d_0. In Fig. 3c, the regions where the solid and dashed lines diverge indicate the activation of the HOCBF constraints. For both Train 1 and Train 2, the average computation time per control step (Steps 4–7 and 10 in Algorithm) is about 0.0028 s, satisfying the real-time requirements of the onboard system.

• *Communication Delay Case*

Now a communication delay of $\tau = \tau_{\max} = 400$ ms is introduced between Train 0 and Train 1 between 50 s and 120 s. Adopting the same setups in the nominal case, the simulation results are shown Fig. 4. When the delay starts at $t = 50$ s, from Fig. 4c we can see that u_1^{ref} switches to cruise. However, the HOCBF constraint b_1 for Train 1 becomes active immediately,

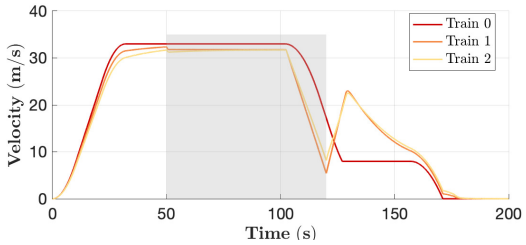

(a) Train velocity profile. During the delayed period, Train 1 takes the conservative following policy, and Train 2 follows its maneuver closely.

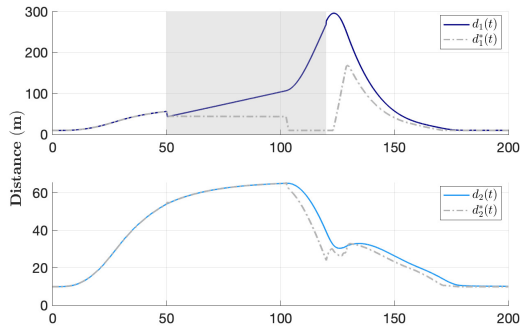

(b) Inter-train distance over time. The actual distance between Train 0 and Train 1 increases due to the delay, reaching nearly 300 m. Train 2 runs closely with Train 1 since there is no delay between them.

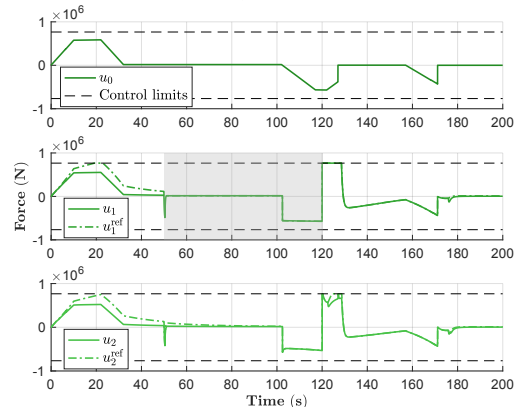

(c) Control force over time. When the communication is restored at 120 s, Train 1 starts accelerating to catch up with Train 0.

Fig. 4: Results of the case with delay $\tau = 400$ ms.

triggering an immediate braking response. Later, when Train 0 begins to decelerate at around $t = 100$ s, u_1^{ref} switches to service braking. Once the delay is resolved, Train 1 quickly catches up with Train 0 as shown in Fig. 4b. A fluctuation in $d_2(t)$ and $d_2^*(t)$ is observed after 120 s, as Train 1 accelerates to reduce the spacing caused by the earlier delay, and then decelerates when Train 0 transitions to a cruising speed. This results in an increase and decrease in $d_2^*(t)$, followed by corresponding adjustments by Train 2.

V. CONCLUSIONS

This study proposes a novel safety control approach for VC following trains based on HOCBFs. A delay-aware reference control force is designed to track the leader's position as closely as possible, while maintaining a minimum safe distance. The RBD-based spacing policy is formally encoded using HOCBFs, which provide safety guarantees. By incorporating the reference force into QPs, each follower computes the optimal traction and braking forces and adjusts its velocity accordingly. Simulation results demonstrate that the proposed controller achieves desirable performance, ensuring safety without compromising close running.

Future work will extend this method to more complex virtual coupling scenarios, incorporate stochastic delay modeling, and design more elaborate mechanisms to mitigate the impact of communication delays on the convoy.

REFERENCES

[1] C. Di Meo, M. Di Vaio, F. Flammini, R. Nardone, S. Santini, and V. Vittorini, "ERTMS/ETCS Virtual Coupling: Proof of Concept and Numerical Analysis," *IEEE Transactions on Intelligent Transportation Systems*, vol. 21, pp. 2545–2556, June 2020.

[2] S. Zhang, P. Huang, and W. Yan, "A data-driven approach for railway in-train forces monitoring," *Advanced Engineering Informatics*, vol. 59, p. 102258, 2024.

[3] T. Schumann, "Increase of capacity on the shinkansen high-speed line using virtual coupling," *International Journal of Transport Development and Integration*, vol. 1, pp. 666–676, 01 2017.

[4] D. Emery, "Enhanced ETCS L2/L3 train control system," in *WIT Transactions on State of the Art in Science and Engineering*, vol. 1, pp. 113–122, WIT Press, 1 ed., June 2010.

[5] B. Ning, "Absolute braking and relative distance braking-train operation control modes in moving block systems," *WIT Transactions on The Built Environment*, vol. 37, 1998.

[6] Y. Liu, D. Ou, Y. Yang, and D. Dong, "A method for maintaining virtually coupled states of train convoys," *Proceedings of the Institution of Mechanical Engineers, Part F: Journal of Rail and Rapid Transit*, vol. 237, no. 2, pp. 243–252, 2023.

[7] Q. Wu, X. Ge, Q.-L. Han, B. Wang, H. Wu, C. Cole, and M. Spiryagin, "Dynamics and control simulation of railway virtual coupling," *Vehicle System Dynamics*, vol. 61, no. 9, pp. 2292–2316, 2023.

[8] C. Liu and Z. Xu, "Multi-agent system based cooperative control for speed convergence of virtually coupled train formation," *Sensors*, vol. 24, no. 13, p. 4231, 2024.

[9] Z. Li, L. Zhong, H. Yang, and L. Zhou, "Distributed cooperative tracking control strategy for virtual coupling trains: An event-triggered model predictive control approach," *Processes*, vol. 11, no. 12, p. 3293, 2023.

[10] Y. Liu, Y. Zhou, S. Su, J. Xun, and T. Tang, "Control strategy for stable formation of high-speed virtually coupled trains with disturbances and delays," *Computer-Aided Civil and Infrastructure Engineering*, vol. 38, pp. 621–639, Mar. 2023.

[11] M. Chen, J. Xun, and Y. Liu, "A coordinated collision mitigation approach for virtual coupling trains by using model predictive control," in *2020 IEEE 23rd International Conference on Intelligent Transportation Systems (ITSC)*, pp. 1–6, IEEE, 2020.

[12] H. Song, W. ShangGuan, W. Qiu, Z. Sheng, and S. S. Harrod, "Two-Stage Optimal Trajectory Planning Based on Resilience Adjustment Model for Virtually Coupled Trains," *IEEE Transactions on Intelligent Transportation Systems*, vol. 24, pp. 15219–15235, Dec. 2023.

[13] J. Park, B.-H. Lee, and Y. Eun, "Virtual Coupling of Railway Vehicles: Gap Reference for Merge and Separation, Robust Control, and Position Measurement," *IEEE Transactions on Intelligent Transportation Systems*, vol. 23, pp. 1085–1096, Feb. 2022.

[14] A. D. Ames, S. Coogan, M. Egerstedt, G. Notomista, K. Sreenath, and P. Tabuada, "Control Barrier Functions: Theory and Applications," in *2019 18th European Control Conference (ECC)*, pp. 3420–3431, June 2019.

[15] W. Xiao and C. Belta, "High-Order Control Barrier Functions," *IEEE Transactions on Automatic Control*, vol. 67, pp. 3655–3662, July 2022.

[16] J. Wang and H. A. Rakha, "Longitudinal Train Dynamics Model for A Rail Transit Simulation System," *Transportation Research Part C: Emerging Technologies*, vol. 86, pp. 111–123, Jan. 2018.

[17] B. P. Rochard and F. Schmid, "A Review of Methods to Measure and Calculate Train Resistances," *Proceedings of the Institution of Mechanical Engineers, Part F: Journal of Rail and Rapid Transit*, vol. 214, no. 4, pp. 185–199, 2000.

[18] A. Lehner, T. Strang, and P. Unterhuber, "Direct train-to-train communications at low uhf frequencies," *IET Microwaves, Antennas & Propagation*, vol. 12, no. 4, pp. 486–491, 2018.